Eight- and nine-photon resonances in multiphoton ionization of xenon

P. Hansch, M. A. Walker, and L. D. Van Woerkom

Department of Physics, The Ohio State University, Columbus, Ohio 43210

We have measured and analyzed the clear emergence of ac-Stark-shifted multiphoton resonances with successive photon orders in xenon. The remarkable quality of our data illustrates the unambiguous evolution through parity-allowed resonances at the eight- and subsequent nine-photon levels. This marks a significant advance in showing that the transient resonance model is valid and strong optical-field ionization remains multiphoton in character at higher intensities. Furthermore, a simple Landau-Zener picture is sufficient to understand the basic principles. [S1050-2947(98)50602-6]

PACS number(s): 32.80.Rm

When atoms are placed in a fixed frequency nonresonant intense laser field, the absorption of multiple photons beyond the ionization limit becomes possible. This process is called above-threshold ionization (ATI) [1,2]. Multiphoton resonances can occur due to light-induced changes in the atom. This was observed by Freeman *et al.* in 1987 for large initial detunings and ultrashort pulse durations [3]. A decade later, interesting physics is still emerging. The purpose of this paper is to directly verify the validity of the transient resonance model for laser intensities large enough to access several sequential photon resonances. We present a complete, high-precision intensity evolution of multiphoton ionization leading to such sequential resonances and extract lifetimes. We are able to describe these features by extending the Landau-Zener curve-crossing theory to include both eight- and nine-photon transitions. Even in the nonperturbative intensity regime the analysis demonstrates that the essential physics of the ionization process remains multiphoton in character.

Between the early studies of low-intensity multiphoton ionization and the current efforts of studying tunneling ionization, little quantitative work has been done investigating the details of ionization in the *intermediate*-intensity range. In particular, there is little experimental work testing the accepted transient resonance model at higher laser intensities. Experimentally, there have only been a few measurements indicating resonance with more than one photon order [4,5]. Other experiments [6,7] were limited in the intensity range and, therefore, were not able to unambiguously follow the emergence of the process. Theoretically, electron spectra and ion yields have been calculated for intensities high enough to observe sequential resonances [8,9].

We have observed a significant enhancement in the ionization rate when reaching intensities high enough to access nine-photon resonances in xenon. Using a three-dimensional calculation we show that the transient resonance picture is valid and supports the observed spectral features. The following effects are observed: (i) The clear evolution from eight- to nine-photon resonances. (ii) A substantial increase in photoelectron signal at the nine-photon resonance intensities. (iii) The nine-photon peaks are narrower than the eight-photon peaks.

In the limit of short pulses, photoelectron spectra exhibit substructure within each ATI order. These peaks can be attributed to multiphoton transient resonances of Rydberg states [3]. After the discovery of transient resonances at low kinetic energies (<5 eV), the interest of the community shifted to the overall shape of the photoelectron spectrum. Semiclassical arguments have proven to be somewhat successful for understanding gross features of the spectral envelope; e.g., the existence of a high-energy plateau with a well-defined cutoff [10–13]. Higher-resolution studies of the noble gases have very recently revealed resonant features within single ATI orders at high kinetic energies [14,15]. The nature of these resonances is still being studied. In support of this effort, one purpose of the present work is to provide detailed knowledge of low-kinetic-energy sequential photon resonances as a foundation for understanding resonant mechanisms at higher energies and laser intensities.

As the laser intensity increases, atomic Rydberg levels as well as the ionization limit shift up by the ponderomotive energy U_p [3,16]. At specific intensities the different Rydberg states shift into resonance with photon harmonics, leading to a strongly enhanced ionization rate. At the instant a resonance occurs, a transient state with initial energy E_i above the ground state produces a photoelectron with kinetic energy $E = m\hbar\omega - IP - (n\hbar\omega - E_i)$, where IP is the field-free ionization potential relative to the ground state, n indicates the harmonic at which the resonance occurs, and m ($>n$) represents the total number of photons absorbed during ionization.

The various Rydberg-state resonances produce electrons that have different kinetic energies, which account for the substructure within each ATI order. Given the resonant nature of this process, photoelectron peaks corresponding to specific transient resonances appear in the kinetic-energy spectra and they do not shift with absolute laser intensity. Therefore, the presence or absence of certain resonances is a good indicator of the overall laser intensity. However, as the intensity increases, other effects may play an important role in determining the photoelectron yield. For example, the large number of photons involved (>8) and the high-intensity ac-Stark shifts of bound levels could create coupling between states, leading to nonponderomotive energy shifts. Calculations have shown this to be the case, although experimental demonstration remains weak [8,17,18]. Thus, it is not obvious that the simple resonance model proposed by Freeman *et al.* [3] is valid at higher intensities. We show that, in spite of the high intensity and many possible cou-

plings, the process remains simple in nature and is dominated by the higher-angular-momentum states.

We have recorded photoelectron time-of-flight spectra of xenon using a Positive Light, Inc. 1-kHz Ti:sapphire laser system, generating 120-fs, 800-nm output pulses with an energy of 700 μJ/pulse. The absolute peak intensity $I_0 = 6.4 \times 10^{13}$ W/cm^2 at the minimum beam waist was held fixed, while spectra over the range $5 \times 10^{12} - 6.4 \times 10^{13}$ W/cm^2 were recorded via intensity-selective-scanning (ISS), which has been described elsewhere [19]. Briefly, only a selected "slice" is exposed to the detector instead of the entire Gaussian focal volume. By scanning the slice along the propagation direction we achieve very precise intensity control and excellent signal-to-noise ratios. Given the kilohertz repetition rate, approximately 1×10^6 laser shots/spectrum have been recorded at static xenon pressures between 1×10^{-7} and 1×10^{-5} Torr.

Figure 1 shows the first ATI order of the photoelectron kinetic-energy spectra for the intensity range of $1.63 \times 10^{13} - 4.68 \times 10^{13}$ W/cm^2. The structure is similar for the other ATI orders; however, differences appear above 12 eV. Each curve is normalized to a common maximum amplitude for better comparison of relative effects. The unprocessed vertical scale increases by a factor of 100 from Fig. 1(a) to Fig. 1(h). The ionization potential for leaving neutral Xe in the $^2P_{3/2}$ single-ion state is 12.127 eV. Given 800-nm photons (1.55 eV), the first parity-allowed multiphoton resonance for the f-series Rydberg states occurs with the eight-photon level.

The emergence of the eight-photon $4f$ resonance is clearly seen as the intensity increases from Fig. 1(a) to 1(b). As the intensity increases beyond the threshold for observing the $4f$ state, the overall signal keeps rising, yet the $4f$ resonance clearly becomes the dominant spectral feature. A broad feature appears in Fig. 1(d) below the $4f$ state for intensities above 2.6×10^{13} W/cm^2. Due to fine structure, the $7p$ state splits into a cluster of six levels with J values ranging from 0 to 3 over an energy range of 0.11 eV. Furthermore, the broadening of this peak toward lower energy indicates nonresonant contributions to the ionization.

Figures 1(f)–1(h) display the sudden emergence of the $6g$ and higher-lying Rydberg g states once the ac-Stark shift brings them into nine-photon resonance. While the eight-photon $4f$-state contribution remains fairly constant in Figs. 1(e)–1(h), the effects of the nine-photon resonances at higher intensities increase dramatically and dominate the spectrum. The onset of these nine-photon resonances occurs at about 3.3×10^{13} W/cm^2, and a similar evolution as with the eight-photon resonances starts over again. Due to the high angular momenta and small quantum defects, the f and g states appear at the same kinetic-energy positions. At our highest intensities we measure a slight redshift relative to the pure ponderomotively positioned states. Estimates using the measured spot size and ionization yields reveal that the observed small shift is possibly due to space charge.

The widths of photoelectron peaks depend on instrumental resolution, the laser bandwidth (inversely on pulse duration), and the short lifetime of the Rydberg states being ionized. We have measured the widths of the f and g states. While all of the g states and high-lying f states have widths
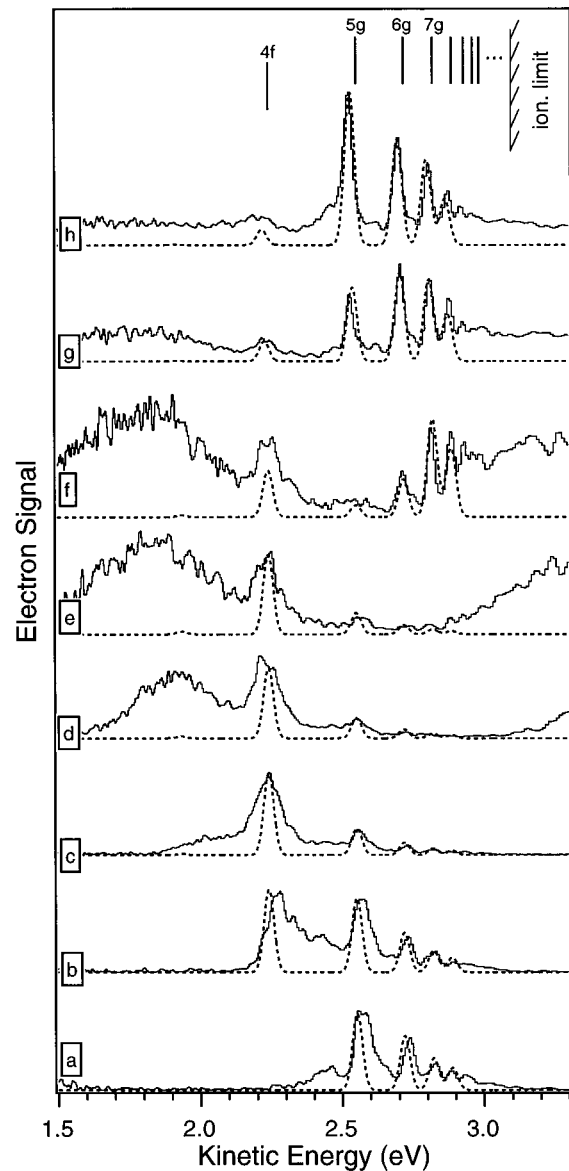
FIG. 1. Photoelectron spectra showing the transition from eight- to nine-photon resonances in xenon using 800 nm light at intensities of (a) 1.66, (b) 1.98, (c) 2.52, (d) 2.85, (e) 3.23, (f) 3.73, (g) 4.12, and (h) 4.68×10^{13} W/cm^2. —, experiment; ---, calculation.

of about 40 meV, the $4f$ and $5f$ states have larger widths of 120 and 74 meV, respectively.

The instrumental resolution is 10 meV at 2.5 eV and the laser bandwidth is approximately 15 meV. For an eight-photon process this yields an inherent spectral width of about 40 meV, indicating a lower limit on the lifetime of the high-lying f and g states of about 16 fs. The $4f$ and $5f$ states, however, exhibit the presence of ionization (lifetime) broadening. Deconvolving the widths using the experimental values, we estimate widths of 113 and 62 meV for the $4f$ and $5f$ levels. This translates into a lifetime of 5.8 fs for the $4f$ state and 10.5 fs for the $5f$ state. Due to the higher angular momentum of the g states and hence less penetration into the core region, the nine-photon features are expected to be narrower and more stable against ionization even though they appear at higher intensities.

Figure 2 displays the peak counts as a function of inten-
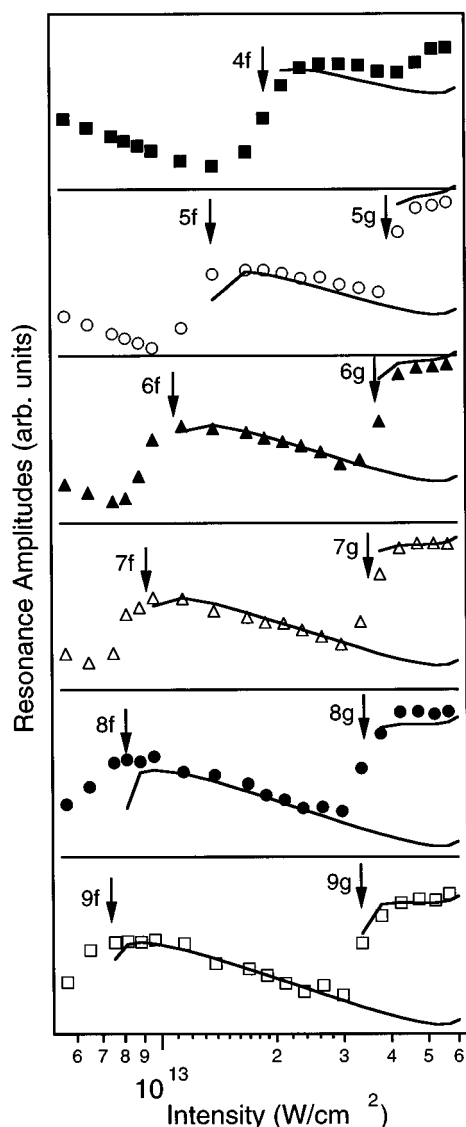
FIG. 2. Resonance peak amplitudes vs intensity. Vertical arrows show the eight- and nine-photon resonance threshold intensities for each state. Symbols are experimental data; solid lines are Gaussian volume contours for f and g states.

sity for the specific kinetic energies associated with the degenerate hydrogenic Rydberg-state resonances for the f and g states. All curves are displayed on a log-log plot. The individual graphs in Fig. 2 have the same amplitude scale and are vertically separated. It is important to recall the difference between the ISS technique and full volume measurements. Traditionally, the ionization signal increases with rising intensity due to volumetric growth. In contrast, the restricted ISS volume can result in a decrease in signal as higher intensities are selected. This effect is evident in the region from 1 to 3×10^{13} W/cm^2 in Fig. 2 where the signal decreases as the Gaussian focal contour is followed. For comparison, the solid lines indicate the Gaussian intensity contours corresponding to each f- and g-state resonance intensity. The data follow the Gaussian contours extremely well.

Figure 2 clearly shows the threshold behavior for each transient resonance as soon as the corresponding resonance

intensity is reached. After a rapid rise the signal follows the Gaussian volumetric behavior until the nine-photon resonance intensities become available. At that point, a dramatic jump in photoelectron signal is observed due to the onset of the g states. Since $n = 5$ is the lowest-lying g state, no higher-order jump can be observed in the $n = 4$ curve. The volumes occupied by intensities above the nine-photon resonance thresholds are clearly smaller than for the eight-photon resonances. Nevertheless, a huge rise in signal occurs when ionizing out of g states. The g state contours in Fig. 2 had to be scaled up by a factor of 300 to account for the increased ionization probability. This demonstrates that the probability for nine-photon ionization exceeds that for the eight-photon process by about two orders of magnitude. This is to be expected due to the nine-photon g-state resonances occurring at about a factor of 3–5 higher intensity.

We have analyzed the evolution of the eight- and nine-photon resonances in the context of multiphoton Landau-Zener theory [7,20–22]. In short, the ground state is dressed in energy with either eight or nine photons to create an avoided crossing with the time-dependent energy levels of the Rydberg states. The ac-Stark shift of the Rydberg states is assumed to be purely ponderomotive. The probability of a multiphoton transition to a particular Rydberg state via adiabatic passage is given by

$$P = 1 - e^{-2\pi V_R^2 \tau_c^2}, \tag{1}$$

where V_R is the coupling strength related to the transition matrix element and τ_c is the resonance time [20]. The coupling strengths depend on the laser intensity *only* through the resonance intensity I_R at which the crossing occurs. One set of V_R's is selected to fit the relative photoelectron peak heights for one intensity slice. The entire evolution is determined from these values and a knowledge of the focal geometry in ISS. The ionization signal due to a single resonance is found by assuming instantaneous ionization from the Rydberg states. Thus, the amplitudes for each resonance in a photoelectron spectrum are constructed by overlapping individual contributions from each state. Saturation effects due to rising and falling edge ionization are also included [20]. A full three-dimensional spatial integration is performed using the geometry of a volume slice for each spectrum.

TABLE I. Coupling strengths V_R and the corresponding resonance intensities I_R for each resonance used in fitting the spectral data in Fig. 1.

State	V_R (fs^{-1})	I_R (10^{14} W/cm^2)
$8f$	5.60(05)	0.081
$7f$	7.60(05)	0.092
$6f$	0.00012	0.109
$5f$	0.00022	0.137
$4f$	0.00057	0.189
$8g$	0.00185	0.340
$7g$	0.00265	0.351
$6g$	0.0032	0.368
$5g$	0.0045	0.396

Calculated photoelectron spectra are shown in Fig. 1 along with the data. Our simple analysis follows the data reasonably well. For simplicity, only the f and g states up to $n = 8$ are included in the mode. We have not included the p or d states since they are not the dominant series in the data. Furthermore, due to our small angular acceptance and the different angular distributions emanating from different resonances, we cannot compare the relative heights with lower-angular-momentum states. The calculated spectra for Figs. 1(g) and 1(h) have been redshifted by approximately 20 meV to account for experimental space charge. Furthermore, each peak in the calculated spectra has an artificial Gaussian $1/e$ half width of 25 meV. Nonresonant processes have not been included in the calculation. The purpose of the calculation is to show the validity of the multiphoton curve-crossing picture for several successive crossings. Future efforts are needed to correctly account for the intensity-dependent widths. It is not necessary to invoke tunneling ionization or sophisticated resonance models to describe the ionization process at these intensities.

Table I shows the values of the coupling strengths and the corresponding resonance intensity for the states included in the analysis. The calculation cannot distinguish different functional forms for the couplings V_R. If the process proceeds via purely perturbative paths, one would expect $(V_R)^2$ to follow an nth-order intensity power law where $n = 8$ or 9. It is possible within the current framework to fit the coupling strengths with an order of nonlinearity between 5 and 9. For any value of n in this range effective cross sections can be found that are consistent with estimates [23].

In conclusion, the clear evolution through parity-allowed resonances at the eight- and subsequent nine-photon levels has been observed. Calculated photoelectron spectra demonstrate the validity of the transient resonance picture near the saturation intensity. The detailed understanding of low-kinetic-energy sequential photon resonances serves as a basis for the study of resonant phenomena at higher energies.

---

[1] P. Agostini, F. Fabre, G. Mainfray, G. Petite, and N. K. Rahman, Phys. Rev. Lett. **42**, 1127 (1979).

[2] Y. Gontier, M. Poirier, and M. Trahin, J. Phys. B **13**, 1381 (1980).

[3] R. R. Freeman, P. H. Bucksbaum, H. Milchberg, S. Darack, D. Schumacher, and M. E. Geusic, Phys. Rev. Lett. **59**, 1092 (1987).

[4] H. Helm and M. J. Dyer, Phys. Rev. A **49**, 2726 (1994).

[5] M. D. Perry, A. Szöke, and K. C. Kulander, Phys. Rev. Lett. **63**, 1058 (1989).

[6] H. Rottke, B. Wolff, M. Brickwedde, D. Feldmann, and K. H. Welge, Phys. Rev. Lett. **64**, 404 (1990).

[7] R. B. Vrijen, J. H. Hoogenraad, H. G. Muller, and L. D. Noordam, Phys. Rev. Lett. **70**, 3016 (1993).

[8] M. Dörr, D. Feldmann, R. M. Potvliege, H. Rottke, R. Shakeshaft, K. H. Welge, and B. Wolff-Rottke, J. Phys. B **25**, L275 (1992).

[9] Y. Gontier and M. Trahin, Phys. Rev. A **46**, 1488 (1992).

[10] M. Lewenstein, K. C. Kulander, K. J. Schafer, and P. H. Bucksbaum, Phys. Rev. A **51**, 1495 (1995).

[11] W. Becker, A. Lohr, and M. Kleber, J. Phys. B **27**, L325 (1994).

[12] P. B. Corkum, Phys. Rev. Lett. **71**, 1994 (1993).

[13] K. C. Kulander, J. Cooper, and K. J. Schafer, Phys. Rev. A **51**, 561 (1995).

[14] M. P. Hertlein, P. H. Bucksbaum, and H. G. Muller, J. Phys. B **30**, L197 (1997).

[15] P. Hansch, M. A. Walker, and L. D. Van Woerkom, Phys. Rev. A **55**, R2535 (1997).

[16] The ponderomotive energy Up is defined in atomic units as $I/4\omega^2$, where I and ω are the laser intensity and frequency, respectively. For 800 nm photons, $Up = 5.98$ eV at 10^{14} W/cm^2.

[17] M. Dorr and R. Shakeshaft, Phys. Rev. A **38**, 543 (1988).

[18] G. N. Gibson, R. R. Freeman, and T. J. McIlrath, Phys. Rev. Lett. **69**, 1904 (1992).

[19] P. Hansch and L. D. Van Woerkom, Opt. Lett. **21**, 1286 (1996).

[20] L. D. Van Woerkom, R. R. Freeman, W. E. Cooke, and T. J. McIlrath, J. Mod. Opt. **36**, 817 (1989).

[21] A. Szöke, J. Phys. B **21**, L125 (1988).

[22] T. J. McIlrath, R. R. Freeman, W. E. Cooke, and L. D. Van Woerkom, Phys. Rev. A **40**, 2770 (1989).

[23] P. Lambropoulos and X. Tang, J. Opt. Soc. Am. B **4**, 821 (1987).